Proc. Natl. Acad. Sci. USA
Vol. 96, pp. 11200–11205, September 1999
Biochemistry

Verification of phylogenetic predictions *in vivo* and the importance of the tetraloop motif in a catalytic RNA

(RNase P/M1 RNA/precursor tRNA/precursor 4.5S RNA)

DANIEL A. POMERANZ KRUMMEL AND SIDNEY ALTMAN*

Department of Molecular, Cellular and Developmental Biology, Yale University, 266 Whitney Avenue, New Haven, CT 06511

Contributed by Sidney Altman, August 3, 1999

ABSTRACT **M1 RNA, the catalytic subunit of *Escherichia coli* RNase P, forms a secondary structure that includes five sequence variants of the tetraloop motif. Site-directed mutagenesis of the five tetraloops of M1 RNA, and subsequent steady-state kinetic analysis *in vitro*, with different substrates in the presence and absence of the protein cofactor, reveal that (*i*) certain mutants exhibit defects that vary in a substrate-dependent manner, and that (*ii*) the protein cofactor can correct the mutant phenotypes *in vitro*, a phenomenon that is also substrate dependent. Thermal denaturation curves of tetraloop mutants that exhibit kinetic defects differ from those of wild-type M1 RNA. Although the data collected *in vitro* underscore the importance of the tetraloop motif to M1 RNA function and structure, three of the five tetraloops we examined *in vivo* are essential for the function of *E. coli* RNase P. The kinetic data *in vitro* are not in total agreement with previous phylogenetic predictions but the data *in vivo* are, as only mutants in those tetraloops proposed to be involved in tertiary interactions fail to complement *in vivo*. Therefore, the tetraloop motif is critical for the stabilization of the structure of M1 RNA and essential to RNase P function in the cell.**

Escherichia coli RNase P is a ribonucleoprotein enzyme composed of a single RNA (M1 RNA) and a single protein (C5 protein) subunit. Both subunits are essential for RNase P function *in vivo*. However, *in vitro*, M1 RNA alone can catalyze the hydrolysis of all the known RNA substrates of RNase P (1, 2), including precursor tRNAs (ptRNAs) and precursors to 4.5S and 10Sa RNAs (2).

Phylogenetic studies of ribosomal RNA led to the identification of recurring secondary structural motifs such as that of the tetraloop (loops of 4 nts) at the turn of an RNA duplex that has, primarily, one of two sequence variations: GNRA or UNCG (where, N = A, C, G or U; R = A or G) (3). The presence of a tetraloop can confer on short model helices an added thermodynamic stability and therefore one role of a tetraloop might be to stabilize an RNA duplex in a functional RNA molecule (4–6). The tetraloop also could serve to stabilize the tertiary structure of an RNA molecule by making specific contact(s) with a distal site in the molecule (an intramolecular interaction) (7–9). Tetraloops also can form intermolecular interactions, for example, by mediating formation of an RNA-protein complex (10).

M1 RNA has several tetraloops in its proposed secondary structure, as do many other RNAs with identifiable function. Specifically, of the eight loops at the turn of RNA helices in M1 RNA, five are tetraloops (one has the sequence UNCG and four have the sequence GNRA; see Fig. 1). It is not clear what function all the tetraloops of M1 RNA serve or whether they are necessary for RNase P function *in vivo*. The M1 RNA tetraloops could, in principle, (*i*) mediate interactions between M1 RNA and the C5 protein, (*ii*) mediate the binding of M1 RNA to some or all of its RNA substrates, or (*iii*) stabilize the conformation of M1 RNA through intramolecular interaction. Extensive phylogenetic analysis of RNase P RNA sequences from eubacteria has led to proposals that three (L9, L12, and L14; see Fig. 1) of the five tetraloops are involved in intramolecular interactions (11, 12). Such proposals should be directly relevant to function *in vivo*, but not necessarily to function *in vitro*. In this study, the five tetraloops of M1 RNA have been altered to investigate their role in RNase P function. We find that two of the tetraloops are critical for effective processing of two different substrates *in vitro*, although the effects differ in a substrate-dependent manner. Only mutants of the three tetraloops implicated by phylogenetic analysis in intramolecular interactions display defective phenotypes *in vivo*.

MATERIALS AND METHODS

Materials. Restriction endonucleases were purchased from New England Biolabs. DNA oligonucleotides were synthesized (solid phase) at the W. M. Keck Biotechnology Resource Laboratory (Yale Univ.). Vent DNA polymerase was purchased from New England Biolabs. T7 RNA polymerase was purchased from Promega; T7 RNA polymerase for large-scale RNA preparation for thermal denaturation experiments was a gift of W. G. Scott (Univ. of California, Santa Cruz). Nucleoside triphosphates were purchased from Amersham Pharmacia Biotech; DNase I was purchased from Worthington; P-10 (G-25) columns were purchased from Boehringer Mannheim; [α-^{32}P]GTP (400 Ci/mmol) was purchased from Amersham Life Science. Spectra/Por dialysis tubing (molecular weight cut-off of 2,000) was purchased from VWR Scientific.

Mutagenesis and Preparation of RNA. pJA2′, which harbors the *rnpB* gene encoding M1 RNA under the control of the phage T7 RNA polymerase promoter, was digested with *Eco*RI and *Hin*dIII to release a fragment with the gene and the upstream promoter. An *Eco*RI restriction site was introduced in the vector pSelect (Promega) upstream of its phage T7 polymerase promoter. This pSelect construct (digested with *Eco*RI and *Hin*dIII) and the pJA2′ *Eco*RI/*Hin*dIII fragment were ligated. The resultant construct (pSelM1) was used as template for site-directed mutagenesis, according to directions provided by Promega. Oligonucleotide sequences used to generate the nine site-directed mutations in *rnpB* are available on request. pSelM1, encoding *rnpB* wild-type or mutation derivatives thereof, was digested with *Fok*I for run-off transcription *in vitro* to generate full-length *E. coli* M1 RNA (377 nts). Plasmids encoding the natural *E. coli* precursors tRNA^{Tyr} (pTyr) and 4.5S RNA (p4.5S) were linearized with *Fok*I and *Sma*I, respectively, for run-off transcription *in vitro*. RNAs then were prepared as described (13). For RNA used in

The publication costs of this article were defrayed in part by page charge payment. This article must therefore be hereby marked "*advertisement*" in accordance with 18 U.S.C. §1734 solely to indicate this fact.

PNAS is available online at www.pnas.org.

Abbreviations: ptRNA, precursor tRNA; p4.5S, precursor 4.5S RNA.

*To whom reprint requests should be addressed. E-mail: sidney.altman@qm.yale.edu.

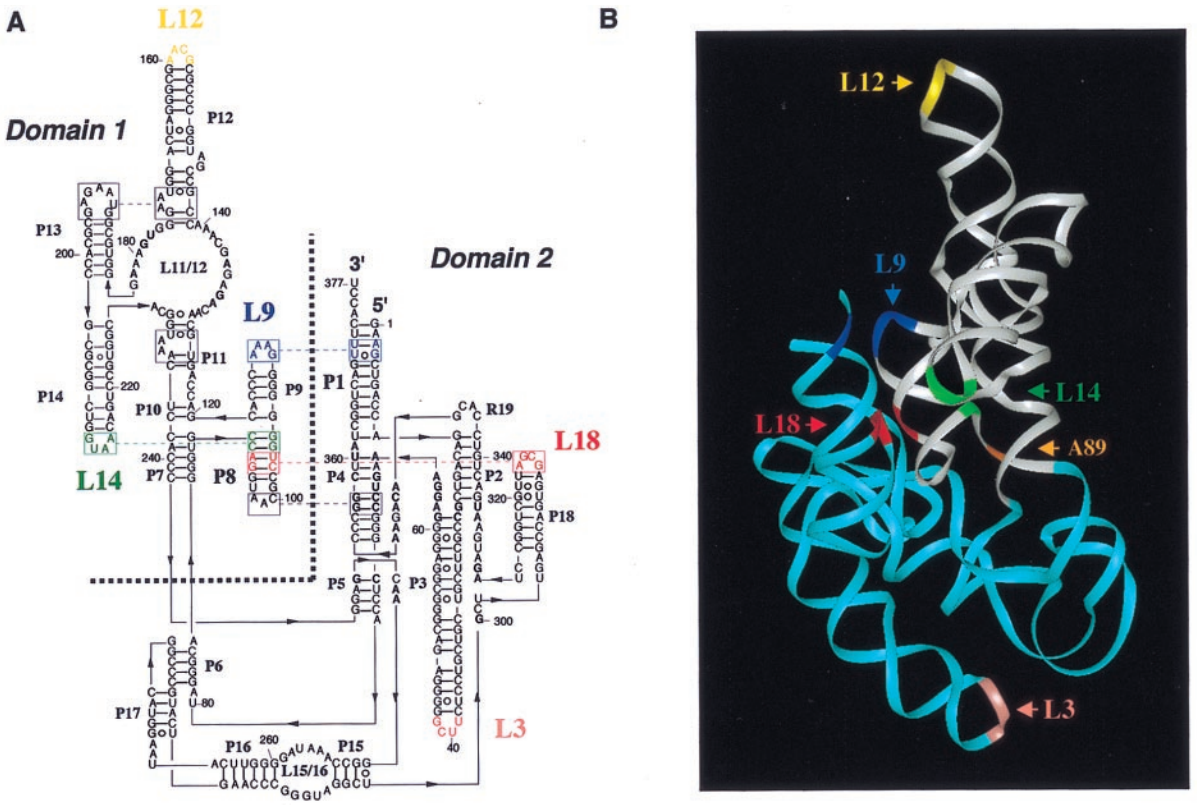

FIG. 1. Proposed Watson-Crick base pairing interactions, indicated by solid lines, and proposed tertiary interactions, indicated by dashed lines, of the secondary structure and three-dimensional computational model of *E. coli* M1 RNA (adapted from ref. 17). (*A*) Secondary structure of *E. coli* M1 RNA: broken line in bold demarcates two proposed independent folding domains of the RNA, domains 1 and 2 (19). Five tetraloops are indicated in color: L3 (pink), L9 (blue), L12 (yellow), L14 (green), and L18 (red) as are their proposed sites of intramolecular interaction (11, 12). (*B*) Three-dimensional computational model of *E. coli* M1 RNA (17). Five tetraloops are indicated in color: L3 (pink), L9 (blue), L12 (yellow), L14 (green), and L18 (red) as are their proposed sites of intramolecular interaction (11, 12). Nucleotide A89 (orange), and domains 1 (white) and 2 (cyan) are highlighted.

thermal denaturation experiments the transcription reaction was scaled up to 1.0 ml. The RNA then was treated as described (13) with the following differences: the RNA was passed through a P-10 column and after precipitation, was resuspended in 100 μl of distilled H_2O and then dialyzed against 200 vol of 6 M urea and 1,000 vol of 1× thermal denaturation buffer (20 mM sodium cacodylate, pH 7.5/400 mM NH_4OAc/1 mM MgOAc).

Substrate RNAs were transcribed in the presence of [α-^{32}P]GTP, electrophoresed on a 7 M urea/denaturing polyacrylamide gel, eluted from the gel by incubation in 1× elution buffer [10 mM Tris·HCl, pH 7.5/1 mM EDTA/100 mM NaCl/0.01% SDS (wt/vol)] at 37°C for 6–8 hr, and then precipitated.

Assays for RNase P Activity. Before assay, wild-type or mutant M1 RNA was renatured in 1× buffer A (50 mM Tris·HCl, pH 7.5/100 mM NH_4Cl/10 mM $MgCl_2$), or, for assays that included C5 protein, in 1× buffer B [10 mM Hepes, pH 7.5/400 mM NH_4OAc/10 mM MgOAc/5% (vol/vol) glycerol] by heating the M1 RNA sample at 65°C for 5 min and then allowing it to cool slowly to room temperature (≈2 hr). The activity of wild-type and mutant M1 RNA was measured at 37°C in 1× buffer A supplemented with 90 mM $MgCl_2$. The activity of the holoenzyme (M1 RNA and C5 protein) also was measured at 37°C in 1× buffer B. The wild-type and mutant M1 RNA and substrate were preincubated for 5 min at 37°C, mixed gently, and placed at 37°C. The time points and the M1 RNA concentrations chosen were selected to obtain measurements in the linear portion of the kinetics of the cleavage reaction. Aliquots were taken at specified times, mixed with 1× volume 9 M urea/dye [0.05% (wt/vol) bromophenol blue, 0.05% (wt/vol) xylene cyanol ff] to quench the reaction, vortexed (5 sec), directly loaded and electrophoresed on denaturing polyacrylamide/7 M urea gels (8% wt/vol). The gels were visualized by use of a PhosphorImager (Fuji), and the reactant and product bands were quantified by using a PhosphorImager program (MACBAS, version 2.0, Fuji). The velocity of the reaction then was estimated from the slope of the curve of substrate cleavage and values for K_M and V_{max} were determined from Eadie-Hofstee plots.

Subcloning and Complementation *in Vivo*. The most proximal natural promoter of *rnpB* directs nearly all its transcription (14). The plasmid used for complementation studies *in vivo* was constructed by digesting pNL3100 (which contains the *rnpB* gene under its natural *E. coli* promoter and terminator) with *Eco*RI and *Sna*BI to generate a single insert. The construct pM1P (*rnpB* upstream of its natural terminator) was digested with *Eco*RI/*Sna*B1, and the vector DNA was isolated. The pNL3100 *Eco*RI/*Sna*BI fragment then was cloned into the pM1P *Eco*RI/*Sna*BI vector. This generates a construct (hereafter referred to as pComM1) with *rnpB* under the control of the most proximal natural *E. coli* rnpB promoter and with a short terminator sequence. The mutant constructs were generated by two rounds of the PCR using the "megaprimer" method (15) (oligonucleotide sequences used to subclone the six site-directed mutations in *rnpB* are available on request). For complementation, *E. coli* strain NHY322 (*rnpA449*), temperature sensitive for RNase P, was transformed with pComM1 constructs. The temperature-sensitive phenotype is complemented by expression of M1 RNA from a high-copy number plasmid (see ref. 16 and references therein). Because NHY322 harbors the tetracycline (Tet) resistance gene and

pComM1 harbors the ampicillin (Amp) resistance gene, pComM1 wild-type and mutant constructs were plated on LB Tet/Amp and grown at both 30°C and 43°C for 48 hr. The ability of the mutants to complement *rnpA49* was assessed based on the number of colonies on plates.

Thermal Denaturation Measurements. RNA (≈26 μg) was renatured in 100 μl of 1× thermal denaturation buffer as described above. The volume then was increased to 1.5 ml (final concentration, 0.145 μM) by addition of 1× thermal denaturation buffer. The RNA was placed on ice, and the denaturation curve was measured within 1 hr. Absorbance at 260 nm was monitored as a function of temperature, which was increased at a rate of 1.0°C/min from 5°C to 92°C, in a CARY 13 UV-VIS spectrophotometer equipped with a five-cuvette thermoelectric controller. The wild-type M1 RNA and mutants L14 and L18 were run simultaneously. Three curves were recorded for each RNA, and a mean of these measurements was taken. Thermal denaturation curves then were normalized at 92°C for comparison, and the first derivative was determined to reveal transitions.

RESULTS

Rationale. Initially, mutants were constructed with the intention to both maintain an added thermodynamic stability that the tetraloop might provide to the RNA helix in which it resides in M1 RNA and to alter the primary sequence and higher-order structure of the tetraloop that might be important for intra- or intermolecular interactions (4–6). Thus, the single UNCG tetraloop (L3) was changed to a GNRA tetraloop and the four GNRA tetraloops (L4, L12, L14, and L18) to UNCG tetraloops (see Table 1). After kinetic characterization of the initial mutants, additional changes were made in certain tetraloops to examine the role of specific residues in the stabilization of the structure of the tetraloop and/or their role in intra- or intermolecular interactions (Table 1). For example, the L9 loop sequence GAAA, was altered to AAAA (L9A111m), a change that removes, *a priori*, the stability provided by base pairing between G1 and A4 of this tetraloop. Likewise, in L14A212m, the first nucleotide of the sequence GUAA was altered to yield a loop sequence of AUAA. In the mutants L14G214m and L18A316m, the third nucleotide was changed to a G or A, respectively, which, in each case, still might participate in an intra- or intermolecular interaction (see Fig. 1 and Table 1).

Examination of a three-dimensional model of *E. coli* M1 RNA indicates that the proposed long-range interactions of tetraloops L9, L14, and L18 are clustered in a region of the RNA on the opposing side of the substrate binding surface (ref. 17; see Fig. 1 *A* and *B*), i.e., they participate in forming the foundation of this surface. Guerrier-Takada and Altman (18) demonstrated that M1 RNA catalytic activity can be reconstituted from various fragments or "sequence modules" of its RNA. A subsequent study further delineated two major folding domains of the RNA, referred to here as domains 1 and 2 (ref. 19; see Fig. 1 *A* and *B*) that are very similar to the modules mentioned above. Massire *et al.* (17) proposed that tetraloops L9, L14, and L18 stabilize the interaction between domains 1 and 2 and, thus, the whole structure of M1 RNA (Fig. 1 *A* and *B*).

Table 1. Sequences of the five M1 RNA tetraloops and the mutations made in these tetraloops

Mutant designation	Wild-type sequence (5′ to 3′) [nucleotides]	Mutant sequence (5′ to 3′)
L3m	UUCG [39–42]	***GAAA***
L9m	GAAA [111–114]	***UCCG***
L9A111m	GAAA [111–114]	***A***AAA
L12m	GCAA [157–160]	***UUCG***
L14m	GUAA [212–215]	***UCCG***
L14A212m	GUAA [212–215]	***A***UA**A**
L14G214m	GUAA [212–215]	GU***G***A
L18m	GCGA [314–317]	***UUCG***
L18A316m	GCGA [314–317]	GC***A***A

Changed nucleotides in loop sequence are in bold and italics.

Catalytic Activity of Wild-Type and Mutant M1 RNA as a Function of Mg^{2+} Concentration. M1 RNA achieves maximum activity at a Mg^{2+} concentration of ≈100 mM in 1× buffer A (20). At this Mg^{2+} concentration tetraloop mutants L3m, L9m, and L12m exhibit wild-type activity (Fig. 2*B* and Table 2). In contrast, in 100 mM Mg^{2+}, L14m and L18m display, relative to wild type, 33% and <10% activity, respectively (Table 2). However, by increasing the Mg^{2+} concentration nearly 2-fold (190 mM) the differences in activity of L14m and L18m relative to wild type are lessened to 80% and 48% activity, respectively. Although L9m and L12m reveal no difference in activity relative to wild type at 100 mM Mg^{2+}, there is a small difference at 20 mM Mg^{2+}: the mutants have 66% and 68% activity, respectively. However, mutants that have this level of relative catalytic activity *in vitro* generally behave as wild type *in vivo* (21) and so these values of catalytic activity are not considered to be significantly different from wild type. At 20 mM Mg^{2+}, L14m and L18m are not active *in vitro* under the conditions used (Fig. 2 and Table 2). Both at 20 mM and 100 mM Mg^{2+}, L3m exhibits wild-type activity (Table 2).

Enzymatic Activity of Wild-Type and Mutant M1 RNA in Absence and Presence of C5 Protein with pTyr as Substrate. L14m and L18m, in the absence of C5 protein in 100 mM Mg^{2+}, exhibit the most significant difference in the kinetics of all tetraloop mutants relative to the wild-type M1 RNA (Table 3). L14m shows a 20-fold increase in both K_M and k_{cat} whereas

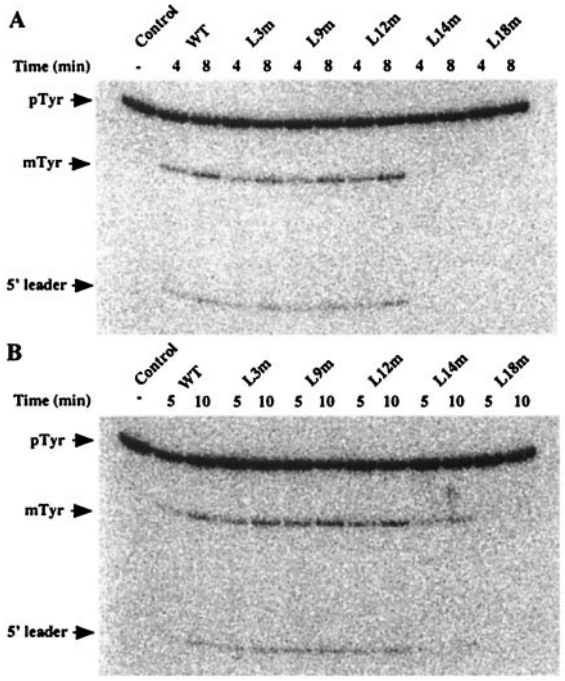

FIG. 2. Enzymatic activity of wild-type (WT) M1 RNA and tetraloop mutants at 20 mM and 100 mM Mg^{2+}. (*A*) Activity of wild-type and tetraloop mutants in 1× buffer A (see *Materials and Methods*) that contains 20 mM Mg^{2+}. Reaction sampled at 4 and 8 min for wild type, as well as five tetraloop mutants. Control is an 8-min sample, under same conditions but in the absence of M1 RNA. (*B*) Activity of wild-type and tetraloop mutants M1 RNA in 1× buffer A that contains 100 mM Mg^{2+}. Reactions sampled at 5 and 10 min. The precursor $tRNA^{Tyr}$ is indicated as pTyr; the product or mature $tRNA^{Tyr}$ is indicated as mTyr; the 5′ leader sequence is indicated as such.

Table 2. Enzymatic activity of wild-type M1 RNA and tetraloop mutants at varying concentrations of Mg^{2+}

	$[Mg^{2+}]$, mM			
	20	37.5	100	190
WT	1.0	1.0	1.0	1.0
L3m	0.93	ND	1.1	ND
L9m	0.66	ND	1.1	ND
L12m	0.68	ND	1.2	ND
L14m	<0.001	0.15	0.33	0.8
L18m	<0.001	0.002	0.07	0.48

Wild-type (WT) M1 RNA and L3m, L9m, and L12m were assayed at a concentration of 10 nM; L14m and L18m were assayed at concentrations of 20 nM and 40 nM, respectively. The pTyr concentration was 100 nM. Values are expressed as a fraction of substrate cleaved per min for mutant enzyme divided by substrate cleaved per minute for the WT M1 RNA. ND, not determined.

L18m shows a 15-fold increase in K_M but not a significant difference in k_{cat}, as compared with wild type. The catalytic efficiency (as judged by the value of k_{cat}/K_M) of L14m is not significantly different from wild type. In contrast, the catalytic efficiency of L18m is approximately 10-fold less than wild type. The origin of the observed kinetic defect of L14m is not caused only by the identity of the first nucleotide of this tetraloop, as L14A212m does not exhibit as significant a difference in either K_M or k_{cat} relative to wild type as does L14m. The third nucleotide of loop L18 does not appear to be the only determinant of the kinetic defect of L18m. However, L18A316m does exhibit changes in both K_M and k_{cat} and, therefore, the mutation in third nucleotide in the loop is a contributing factor to the kinetic defects of L18m.

The addition of C5 protein to assays performed in 10 mM Mg^{2+} changes the kinetics of L14m and L18m such that they are not very significantly different from the wild type (Table 3). In the presence of C5 protein in 10 mM Mg^{2+}, as well in its absence in 100 mM Mg^{2+}, the kinetics of the tetraloop mutants L3m, L9m, L9A111m, L12m, and L14G214 are not very different from wild type. L18A316m has a lower K_M and k_{cat} relative to wild-type M1 RNA, therefore the ratio of the two parameters (the catalytic efficiency) is about the same as that of the wild type.

Enzymatic Activity of Wild-Type and Mutant M1 RNA in Absence and Presence of C5 Protein, with p4.5S as Substrate. There are distinct differences in the kinetics of processing of p4.5S from those with pTyr for the tetraloop mutants in both the presence and absence of the C5 protein (Table 4). In the presence of the C5 protein in 10 mM Mg^{2+}, L9m, which has wild-type activity with pTyr as substrate, exhibits a decrease in both K_M and k_{cat} relative to wild type with p4.5S as substrate. Under the same conditions with p4.5S as substrate, L18m, as well, has a lower K_M and k_{cat} relative to wild type. L14m in the presence of C5 protein exhibits both an increase in K_M and k_{cat}, as was observed in the kinetics of the processing of pTyr in the absence of C5 protein (Table 4). The kinetic defects of L14m and L18m also are reflected in initial velocity measurements made in the absence of C5 protein in 100 mM Mg^{2+} (Table 4). L18m is not active under these conditions. In contrast, L14m is highly active, showing an apparent gain in function in the processing of p4.5S, the opposite of what was found with pTyr as its substrate. L3m, L9m, and L12m exhibit wild-type-like activity.

Table 4. Kinetic parameters of wild-type M1 RNA and tetraloop mutants in the presence and absence of C5 protein with *E. coli* precursor 4.5S RNA as substrate

	M1 RNA	RNase P		
	V_o	K_M, nM	k_{cat}, min^{-1}	k_{cat}/K_M, $min^{-1}{\cdot}nM^{-1}$
WT	1.0	375 ± 87	63 ± 13	0.17 ± 0.05
L3m	0.9	431 ± 210	33 ± 13	0.08 ± 0.05
L9m	1.1	98 ± 42	13 ± 3	0.13 ± 0.03
L12m	0.9	273 ± 67	35 ± 8	0.13 ± 0.01
L14m	2.5	2486 ± 550	300 ± 88	0.12 ± 0.02
L18m	<0.1	87 ± 32	6 ± 1	0.07 ± 0.03

For M1 RNA assays in 100 mM Mg^{2+}, the concentrations of wild-type (WT) M1 RNA, L3m, L9m, L12m, L14m, and L18m were 0.3 μM; the concentration of p4.5S was 10 μM. V_o, % substrate cleaved/min. For RNase P assays in 10 mM Mg^{2+}, M1 RNA WT and mutants at a concentration of 0.4 nM was mixed with 10-fold excess of C5 protein (4.0 nM), and incubated 5 min at 37°C; the concentration of p4.5S was in the range 15 nM to 3.8 μM (7–9 substrate concentrations).

Complementation *in Vivo*. Enzymatic activity assays at 20 mM Mg^{2+} revealed a small decrease relative to wild type for L9m and L12m (Table 2). A previous study with several mutants of M1 RNA had indicated that a small difference in activity, such as we observe for L9m and L12m, is not predictive of failure to complement *in vivo* (21). However, we observe that L9m is unable to complement a temperature-sensitive mutant defective in RNase P activity at the nonpermissive temperature (Table 5). This result shows that the results of kinetic studies *in vitro* do not necessarily reflect

Table 3. Kinetic parameters of wild-type M1 RNA and tetraloop mutants in the presence and absence of C5 protein with the *E. coli* precursor $tRNA^{Tyr}$ as substrate

	M1 RNA			RNase P		
	K_M, nM	k_{cat}, min^{-1}	k_{cat}/K_M, $min^{-1}{\cdot}\mu M^{-1}$	K_M, nM	k_{cat}, min^{-1}	k_{cat}/K_M, $min^{-1}{\cdot}nM^{-1}$
WT	45 ± 9	0.1 ± 0.01	2.2 ± 0.5	44 ± 15	25 ± 5	0.6 ± 0.2
L3m	36 ± 12	0.12 ± 0.01	3 ± 1	124 ± 22	50 ± 8	0.4 ± 0.1
L9m	32 ± 20	0.17 ± 0.03	5 ± 3	69 ± 18	30 ± 5	0.4 ± 0.1
L9A111m	94 ± 59	0.29 ± 0.03	3 ± 2	124 ± 29	43 ± 8	0.3 ± 0.1
L12m	100 ± 50	0.21 ± 0.04	2 ± 1	109 ± 29	33 ± 8	0.3 ± 0.1
L14m	844 ± 149	2.1 ± 0.4	2.5 ± 0.6	127 ± 32	30 ± 8	0.24 ± 0.08
L14A212m	106 ± 27	0.7 ± 0.1	7 ± 2	147 ± 23	38 ± 5	0.26 ± 0.05
L14G214m	ND	ND	ND	49 ± 11	23 ± 3	0.5 ± 0.1
L18m	679 ± 120	0.15 ± 0.03	0.2 ± 0.1	38 ± 10	9 ± 1	0.23 ± 0.07
L18A316m	212 ± 79	0.9 ± 0.3	4 ± 2	10 ± 4	6 ± 11	0.6 ± 0.1

For M1 RNA assays in 100 mM Mg^{2+}, the concentrations of wild-type (WT) M1 RNA, L3m, L9m and L12m were 10 nM, L14m was 20 mM, and L18m was 30 nM; pTyr concentration was in the range of 40 nM to 200 nM (7–9 substrate concentrations). Substrate concentrations greater than 200 nM result in substrate inhibition of WT M1 RNA activity. For RNase P assays in 10 mM Mg^{2+}, M1 RNA WT and mutants at a concentration of 0.4 nM was mixed with a 10-fold excess of C5 protein (4.0 nM), and incubated 5 min at 37°C. The procedure then followed was as that described (see *Materials and Methods*) with the concentration of pTyr in the range of 10 nM to 1.3 μM (6–9 substrate concentrations). ND, not determined.

Table 5. Results of complementation studies of wild-type (WT) M1 RNA and tetraloop mutants

pSelM1	Complementation
WT	++++
L3m	++++
L9m	−
L9A111m	+
L12m	++++
L14m	−
L18m	−

The mutants are classified by their ability to complement *E. coli* NHY322 *A49* at 43°C; ++++, indicates complementation of NHY322, *A49*; +, partial complementation; −, does not complement.

functional capability of RNase P *in vivo*. The G to A change in the L9 tetraloop (L9A111m) complements inefficiently: it does allow the growth of about one-fourth the number of colonies compared with wild-type RNase P at the nonpermissive temperature (43°C; Table 5). L3m and L12m complement *in vivo* but neither L14m nor L18m do, all in agreement with the results of kinetic studies *in vitro* (Table 5).

Thermal Denaturation Studies. Tetraloop mutants L14m and L18m were selected for thermal denaturation studies because of their defects in the processing of both pTyr and p4.5S. Thermal denaturation of wild-type M1 RNA in 1× thermal denaturation buffer that contains either 10 mM or 100 mM Mg^{2+} does not reveal certain well-defined transitions that are observable in 1 mM Mg^{2+} (data not shown). Therefore, thermal denaturation curves of wild-type M1 RNA and mutants L14m and L18m were recorded in 1 mM Mg^{2+}. We anticipated that any differences in thermal denaturation would be accentuated at this low Mg^{2+} concentration because relatively low concentrations of Mg^{2+} can reveal defects in function *in vitro* masked at higher concentrations (see Table 2).

It is apparent from the absorbance versus temperature profiles that a difference exists among wild-type M1 RNA and L14m and L18m, as well as between the two mutants themselves (Fig. 3*A*). The first derivative of the thermal denaturation curve of wild-type M1 RNA exhibits transitions at ≈57°C, ≈77°C, and ≈82°C (Fig. 3*B*). We note that activity of wild-type M1 RNA reaches a maximum at ≈50–55°C (Fig. 3*B Inset*), corresponding approximately to a transition at ≈57°C in the curve of first derivatives of the RNAs. The most pronounced differences from wild type in the first derivative of the thermal denaturation curves and the mutants are at ≈77°C and ≈82°C (Fig. 3*B*).

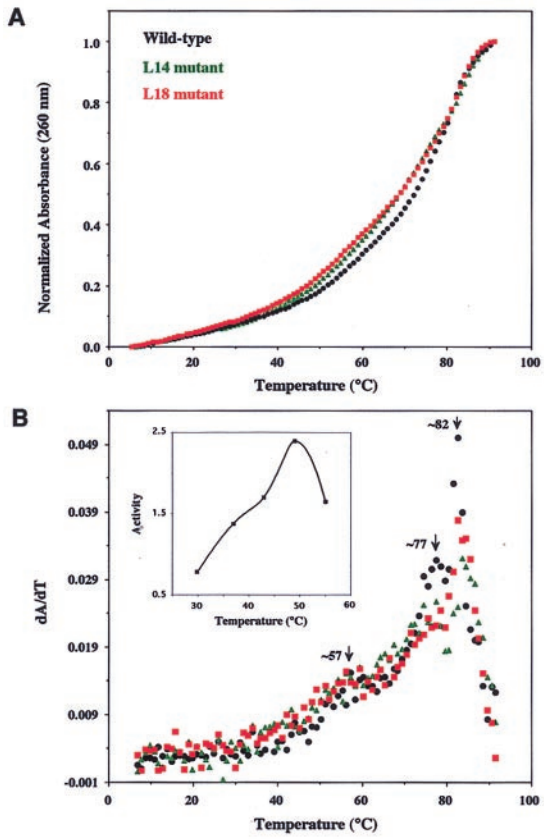

FIG. 3. Thermal denaturation profiles of wild-type M1 RNA and tetraloop mutants L14m and L18m. (*A*) Thermal denaturation profile of wild-type M1 RNA (black) and tetraloop mutants L14m (green) and L18m (red), expressed as normalized absorbance versus temperature. (*B*) First derivative of thermal denaturation profiles of wild-type M1 RNA (black) and tetraloop mutants L14m (green) and L18m (red). Structural transitions are noted at ≈57°C, ≈77°C, and ≈82°C. (*Inset*) Activity of wild-type M1 RNA as a function of temperature. To measure activity as a function of temperature, wild-type M1 RNA (5 nM) and pTyr (100 nM) were incubated at the desired temperature for 5 min, separately, before being mixed in the reaction mixture (see *Materials and Methods*).

DISCUSSION

Phylogenetic Predictions. Phylogenetic studies of eubacterial RNase P RNA sequences have been used to identify covariation of nucleotides distant from each other in sequence space (11, 12). This has led to predictions of long-range interactions involving three of the five tetraloops of *E. coli* M1 RNA: L9 to base pairs 3/371:4/370 of helix P1; L14 to base pairs 94/108:95/107 of helix P8; and L18 to base pairs 96/106:97-105 of helix P8 (11, 12). The proposed interactions do not all involve standard Watson-Crick base pairing, thereby making it difficult to understand the detailed nature of these long-range interactions. The three long-range interactions are clustered in space in helices P8/P9 of *E. coli* M1 RNA (see Fig. 1*B*). The P8/P9 region of *E. coli* M1 RNA appears to be highly dynamic in structure. It undergoes a change in conformation upon binding of certain substrates and its integrity is important for the function of the enzyme as determined by the phenotypes of mutations in this general region (22–24). It is also of interest that the L14 tetraloop becomes accessible to chemical probing as a consequence of a mutation in helix P7 (G89:C240) (ref. 25, see Fig. 1*B*). The tertiary interactions in this region of M1 RNA (helices P7-P9), which is at an interface of the two major independent folding domains of the RNA, may be highly cooperative and are undoubtedly complex. For example, examination of the three-dimensional model of M1 RNA shows that the base pair G89/C240 in helix P7 can stabilize the site of interaction in P8 of the L14 tetraloop (ref. 12; see Fig. 1*B*).

M1 RNA Function *in Vitro*. Data from studies of enzyme kinetics, thermal denaturation experiments, and complementation *in vivo* led us to propose that the L14 and L18 tetraloops have a significant role in determining M1 RNA structure and, consequently, function. The L14 and L18 tetraloop mutants cleave a ptRNA substrate less efficiently than wild-type M1 RNA in a fashion that varies as a function of Mg^{2+} concentration: the discrepancy with wild-type cleavage ability decreases with increasing concentration of Mg^{2+} and is accentuated in low concentrations of Mg^{2+} as one would expect if the tetraloops play a role in stabilizing the structure of M1 RNA. Furthermore, L14m and L18m do exhibit thermal denaturation curves different from wild type, most demonstrably at ≈55°C, ≈77°C, and ≈82°C.

It is apparent from the kinetic data that both the L14 and L18 tetraloops are important for binding of M1 RNA to a ptRNA. The L14 and L18 tetraloop mutants both have increases in K_M. Only the L14m has a change in k_{cat}, an increase in the catalytic rate constant. As the rate-limiting step of the

reaction of wild-type M1 RNA is product release, an increase in k_{cat} could be indicative of a decrease in the affinity of the enzyme for the product as well, albeit this has not yet been proved for the mutant. However, only the L18 mutant has an overall defect in catalytic efficiency, as a consequence of a structural perturbation that affects ptRNA binding. Consistent with our observations regarding the role of L18, lead ion probing experiments show that the fourth base of the L18 tetraloop is important for maintaining *E. coli* M1 RNA structure (26). In addition, modifications in this tetraloop and in the proposed site of its intramolecular interaction (the P8 helix) disrupt tRNA binding (26).

The L14 and L18 tetraloop mutants have totally different effects with p4.5S as substrate as compared with those with pTyr as substrate. L14m with p4.5S as substrate in the presence of C5 protein exhibits the same changes in K_M and k_{cat} as it does with a ptRNA as substrate. However, similar changes are observed for the ptRNA substrate in the absence of C5 protein. C5 protein cannot compensate for the effect of this tetraloop mutation on the kinetic parameters of M1 RNA with p4.5S. L18m also differs in the kinetics of cleavage with p4.5S as compared with pTyr in the presence of C5 protein (Table 4). With L18m, there is a decrease in K_M and a decrease in k_{cat} in the processing of p4.5S. The L18m holoenzyme forms a "tighter" complex with p4.5S than does wild-type RNase P.

M1 RNA, lacking nucleotides 94–204, is unable to catalyze the hydrolysis of pTyr but it does cleave p4.5S when it is part of the holoenzyme complex (19). Obviously, nucleotides 94–204 are part of a domain of M1 RNA that is critical in the processing of ptRNA. All the tertiary interactions discussed above are disrupted in the large deletion mutant. However, disruption of the putative interaction of L14 with P8 alone, an interaction that, *a priori*, is important for stabilizing the domain encompassing nucleotides 94–204, increases the observed rate of processing of p4.5S but decreases the rate of processing of the ptRNA. These data, together, appear to suggest that disrupting the presumptive "L14/P8" interaction or the connection of domain 1 with domain 2 alters the structure of M1 RNA in a way that enables the enzyme to enhance cleavage of a p4.5S-like substrate, as determined previously (18).

Holoenzyme Function *in Vitro* and *in Vivo*. A significant test of the importance of a given structural motif in M1 RNA would be to assess its necessity for the function of the enzyme both *in vivo* and *in vitro*. The comparison also would be a test of the validity of predictions based on phylogenetic analysis. Phenotypes of mutations, including tetraloop mutations, in M1 RNA that have a deleterious effect on its activity can be "overcome" by C5 protein *in vitro* (21). The kinetic data for M1 RNA alone *in vitro* do suggest that the L14 and L18 tetraloops are important for function of M1 RNA and the implications for these mutants *in vivo* are confirmed by complementation tests. The L3, L9, and L12 mutants show no significant diminishment of function *in vitro*. However, L9m cannot complement a strain thermosensitive in RNase P function *in vivo*. Therefore, there is a discordance in this case between function *in vitro* and *in vivo*. The mutants (L9m, L14m, and L18m) that exhibit defects *in vivo* are exactly those predicted by phylogenetic analysis to be involved in tertiary interactions (11, 12).

We are grateful to Dr. D.M. Crothers and J. Carruthers for guidance with the thermal denaturation experiments. D.A.P.K. thanks Dr. E. Westhof for encouragement and advice. We thank members of our lab, in particular Drs. V. Gopalan and C. Guerrier-Takada for advice. We also thank Dr. B. Schmid for assistance with figures. Research in S.A.'s laboratory is supported by U.S. Public Health Service Grant GM-19422 and Human Frontier Science Program Grant RG0291. D.A.P.K. acknowledges the support of a National Institutes of Health predoctoral training grant to Yale University.

1. Guerrier-Takada, C., Gardiner, K., Marsh, T., Pace, N. & Altman, S. (1983) *Cell* **35,** 849–857.
2. Altman, S. & Kirsebom, L. (1999) in *The RNA World*, eds. Gesteland, R. F., Cech, T. R. & Atkins, J. P. (Cold Spring Harbor Lab. Press, Plainview, NY), pp. 351–380.
3. Woese, C. R., Winker, S. & Gutell, R. R. (1990) *Proc. Natl. Acad. Sci. USA* **87,** 8467–8471.
4. d'Aubenton-Carafa, Y., Uhlenbeck, O. C. & Tinoco, I., Jr. (1988) *Proc. Natl. Acad. Sci. USA* **85,** 1364–1368.
5. Cheong, C., Varani, G. & Tinoco, I., Jr. (1990) *Nature (London)* **346,** 680–682.
6. Heus, H. A. & Pardi, A. (1991) *Science* **253,** 191–194.
7. Jaeger, L., Michel, F. & Westhof, E. (1994) *J. Mol. Biol.* **236,** 1271–1276.
8. Murphy, F. L. & Cech, T. R. (1994) *J. Mol. Biol.* **236,** 49–63.
9. Cate, J. H., Gooding, A. R., Podell, E., Zhou, K., Golden, B. L., Kundrot, C. E., Cech, T. R. & Doudna, J. A. (1996) *Science* **273,** 1678–1685.
10. Gluck, A., Endo, Y. & Wool, I. G. (1992) *J. Mol. Biol.* **226,** 411–424.
11. Brown, J. W., Nolan, J. M., Haas, E. S., Rubio, M. A. T., Major, F. & Pace, N. R. (1996) *Proc. Natl. Acad. Sci. USA* **91,** 3001–3006.
12. Massire, C., Jaeger, L. & Westhof, E. (1997) *RNA* **3,** 553–556.
13. Gopalan, V., Baxevanis A. D., Landsman, D. & Altman, S. (1997) *J. Mol. Biol.* **267,** 818–829.
14. Lee, Y., Ramamoorthy, R., Park, C.-U. & Schmidt, F. J. (1989) *J. Biol. Chem.* **264,** 5098–5103.
15. Sarkar, G. & Sommer, S. S. (1990) *BioTechniques* **8,** 404–407.
16. Kirsebom, L. A., Baer, M. F. & Altman, S. (1988) *J. Mol. Biol.* **204,** 879–888.
17. Massire, C., Jaeger, L. & Westhof, E. (1998) *J. Mol. Biol.* **279,** 773–779.
18. Guerrier-Takada, C. & Altman, S. (1992) *Proc. Natl. Acad. Sci. USA* **89,** 1266–1270.
19. Loria, A. & Pan, T. (1996) *RNA* **2,** 551–563.
20. Guerrier-Takada, C., Haydock, K., Allen, L. & Altman, S. (1986) *Biochemistry* **25,** 1509–1515.
21. Lumelsky, N. & Altman, S. (1988) *J. Mol. Biol.* **202,** 443–454.
22. Guerrier-Takada, C., Lumelsky, N. & Altman, S. (1989) *Science* **246,** 1578–1584.
23. Knap, A. K., Wesolowski, D. & Altman, S. (1990) *Biochimie* **72,** 779–790.
24. Pomeranz Krummel, D. A. & Altman, S. (1999) *RNA* **5,** 1021–1033.
25. Shiraishi, H. & Shimura Y. (1989) *EMBO J.* **7,** 3817–3821.
26. Heide, C., Pfeiffer, T., Nolan, J. M. & Hartmann, R. K. (1999) *RNA* **5,** 102–116.